

# Quantum Chaos, Localization and Tunneling: Microwave Experiments on Model Geometries

S. Sridhar

Physics Department, Northeastern University,  
360 Huntington Avenue, Boston, MA 02115.

April 4, 2000

Lectures presented at the XII Physics Summer School : Quantum and Classical Chaos  
Jan.11 - 22, 1999, Australian National University, Canberra.

## Abstract

Microwave experiments using 2-D billiard geometries are a precise test of basic issues in Quantum Chaos, Localization and Tunneling. In closed chaotic geometries, analysis of eigenvalue statistics yield good agreement with Random Matrix Theory. A unique aspect of the experiments is the ability to directly measure eigenfunctions. The influence of periodic orbit scarring in chaotic eigenfunctions is directly demonstrated. Disordered microwave billiards are a text-book model system for studying the quantum properties of a single particle in a disordered potential. Localization is directly observed in eigenfunctions of the disordered billiards. Statistical properties of disordered eigenfunctions deviate from universal behavior due to localization. These statistical properties are in good agreement with predictions from nonlinear-sigma models, although many challenges for further theoretical understanding remain. The experiments can also probe open systems, in terms of the quantum resonances and escape rate of a fractal repeller.

The study of the quantum manifestations of classical chaos is an active area of current research known as Quantum Chaos. Recent years have seen significant developments in theoretical approaches paralleled by remarkable experimental observations in a variety of sub-fields of physics.

The use of microwave systems to study model problems in Quantum Chaos has proven to be a very fruitful and insightful approach. This paper summarizes the principal results obtained from such experiments performed at the author's laboratory. Further details are available in the publications which are listed in the reference section [1] - [16]. The principal topics addressed here are :

1. Universal features of the Eigenvalue Statistics of Chaotic Billiard Cavities.
2. Eigenfunctions of Chaotic Billiards : Scars and Statistics.
3. Eigenfunctions of Disordered Billiards : Localization.
4. Open Systems : Resonances and Decay of a Fractal Repeller.
5. Tunneling.

## A: Experimental Details

The experiments utilize “thin” microwave cavities, in which below a cutoff frequency, the 2-D scalar limit of the Maxwell-Helmholtz wave equation applies, and the correspondence to the Schrödinger equation is exact. For a cavity of arbitrary cross-section in the  $x-y$  plane but uniform along the  $z$ -direction, the  $z$ -component of the wave vector is quantized as  $k_z = p\pi/d$ , where  $p$  is an integer and  $d$  is the cavity thickness along the  $z$ -axis. Maxwell’s equations then reduce to :

$$[\nabla^2 + (k^2 - (p\pi/d)^2)] \{E_z, B_z\} = 0 \quad (1)$$

where  $\nabla$  is the 2-D Laplacian operator. Of course the  $EM$  field is a vector field, however a special case occurs for the *Transverse Magnetic (TM)* modes for which  $B_z = 0$ , and further when  $p = 0$ . In this limit, Eq. 1 reduces to the Schrödinger equation,  $(\nabla^2 + k^2)\Psi = 0$ , where  $\Psi \longleftrightarrow E_z$ . This limit can be experimentally achieved by confining measurements to the frequency range  $f < f_c = c/d$ . For  $d = 6\text{ mm}$ , the cutoff frequency  $f_c = 25\text{ GHz}$ , and for all frequencies lower than  $f_c$ , the correspondence between the Schrödinger and Maxwell wave equations is exact in the thin 2-D cavities.

Cavities are fabricated with the 2-dimensional cross-section cut out from 6mm thick Copper sheets, and placed between two Copper plates. Coupling to the cavities is accomplished by loops terminating coaxial cables - the loops couple to the microwave magnetic fields at the perimeter. The cavity response is examined using an HP 8510 Network Analyzer (ANA). The eigenvalue spectrum is obtained from the resonances observed in the transmission spectrum, with the energy eigenvalues  $E_n$  obtained from the resonant eigenfrequencies  $f_n$  using  $E_n = f_n^2$ . By using appropriate care, in particular coupling at several locations, it is possible to observe the first 1000 or so levels of the spectrum, without any missed levels. Thus although the finite conductivity of the Copper walls leads to broadened resonances, it is not necessary to use superconducting cavities in order to carry out reliable experiments on eigenvalue statistics. A photograph of the experimental setup is shown in Fig.1.

One of the important and unique features of the experiments is the ability to directly measure eigenfunctions. This method, first devised by the author [1, 2], utilizes the perturbation of the cavity resonance by a small metallic perturber. Placing the perturber at coordinates  $(x, y)$  in the cavity leads to a shift of the resonance frequency  $\Delta f_n(x, y) = -\beta |\Psi_n^2(x, y)|$ , from which the eigenfunction density  $|\Psi_n^2(x, y)|$  can be directly determined by measuring the frequency shift  $\Delta f_n(x, y)$ . This method enables the direct visualization of eigenfunctions without inserting a probe into the cavity.

## B: Eigenvalue Statistics of Chaotic Billiards

An important notion in quantum chaos is that of universality, according to which the statistical properties of quantum parameters such as eigenvalue spectra and eigenfunctions, obey universal behavior independent of the details of the Hamiltonian, but determined instead by general symmetry properties. Quantitative calculations of universal behavior are feasible using Random Matrix Theory, which has been studied extensively following the early work of Wigner, Dyson and Mehta [18]. The applicability of Random Matrix Theory to Quantum Chaotic systems, was first proposed by Bohigas, Giannoni and Schmidt [19], and has since received extensive experimental confirmation.

The microwave experiments have yielded precision tests of eigenvalue statistics [4]. Experiments were carried out on chaotic Sinai billiard and Sinai-Stadium cavities. Approximately 600-1000 levels were obtained for each geometry. Careful measurement using several probe locations ensure that there were no missed levels. The eigenvalue spectra were analyzed in terms of several statistical measures such as, the nearest-neighbor spacing statistics  $P(s)$ , as well as longer range correlations such as the level rigidity  $\Delta_3(L)$ . To measure the consequences in the time domain, we also study the Fourier transform of the spectral auto-correlation  $\ll P(\tau) \gg$ , which can be interpreted as the survival probability.

The spacing statistic  $P(s)$  clearly shows the level repulsion characteristic of quantum chaotic systems. The results are in quantitative agreement with the Wigner-Dyson formula from RMT - small deviations can be attributed to periodic orbits. The results for  $\Delta_3(L)$  are found to depend crucially on the nature of the periodic orbits present in the chaotic geometry, particularly the presence of marginally stable Periodic Orbits (PO). For the Sinai billiard,  $\Delta_3(L)$  follows GOE upto  $L \sim 10$ , above which a linear rise deviating from GOE is observed. This linear rise is due to stronger fluctuations in the spectrum arising from the presence of the marginally stable PO. Excellent agreement with GOE predictions of RMT is obtained only after excluding such PO, as we demonstrated for the Sinai-stadium billiard [4].



Figure 1: Photograph of the experimental setup at Northeastern for studying quantum chaos in microwave systems

A striking signature of quantum chaos that is observed in the survival probability  $\ll P(\tau) \gg$  is the so-called “correlation hole”. The correlation hole appears as values of  $\ll P(\tau) \gg$  below the asymptotic value of  $\ll P(\tau) \gg_{\tau \rightarrow \infty} \rightarrow 0.25$  for values of  $\tau < 1/\Delta E$ , where  $\Delta E$  is the nearest-neighbor level spacing. The correlation hole may be regarded as another manifestation of level repulsion, and is only observed in quantum chaotic spectra. Quantitative agreement was obtained between experimental results for the survival probability and calculations based upon RMT [4].

Experiments were also carried out on pseudo-integrable (PI) L-billiards. For both eigenvalue and eigenfunctions properties, the results for the PI billiards fall between those of integrable and chaotic geometries. Further details for the L-billiard are described in ref. [11].

### C: Eigenfunctions of Chaotic Billiards : Scars and Statistics

The eigenfunctions of chaotic geometries reveal a fascinating complexity. Unlike integral systems, where each eigenfunction can be spectroscopically labeled by quantum numbers for the various integrals of the classical motion, such as the energy  $E_n$  and the  $(p, q)$  quantum numbers for the momentum for the rectangle billiard, the only quantum number that survives for the chaotic geometry is the energy eigenvalue. A proper quantitative understanding of chaotic wavefunctions is a continuing endeavor of quantum chaologists.

A major step in this direction was the recognition by Heller [20] that periodic orbits play an important role in chaotic wavefunctions in terms of the presence of “scars”, which represent localization of intensities along isolated PO. While scars were observed in numerical simulations and were implicated in a variety of

phenomena in atomic physics, the first direct experimental visualization of scars was reported in a Sinai billiard microwave cavity by the author [1].

The science of “scarology” in experimental wavefunctions has not progressed much beyond visual identification of scars. More quantitative tests of scarring which have been proposed have been attempted on our wavefunctions, but the results are not conclusive. The characterization of chaotic wavefunctions in terms of classical phase space structures such as PO, as well as others such as homoclinic orbits, is very important and will surely be the subject of continuing study.

An alternative approach to analyzing chaotic wavefunctions is a statistical one paralleling the analysis of chaotic eigenvalue spectra. We have demonstrated that chaotic eigenfunctions display universal statistical properties in good agreement with RMT [8, 9].

The most basic statistical measure is the density distribution  $P(|\Psi|^2)$ , which is a histogram of the density values averaged over many levels. This distribution was shown [8] to be in excellent agreement with the famous Porter-Thomas distribution  $P(|\Psi|^2) = 1/\sqrt{2\pi|\Psi|^2} \exp(-|\Psi|^2/2)$ , demonstrating the universality of this distribution, which is also observed in nuclear and other systems. There are small deviations at large  $|\Psi|^2$  from the P-T distribution due to the presence of PO, with the greatest deviations arising again from bouncing-ball or marginally stable PO. This situation is similar to the deviations mentioned earlier from the Wigner-Dyson form for  $P(s)$  also due to b-b PO.

Spatial correlations of the chaotic eigenfunctions were also studied. The density-density correlation  $P_2(r) = \ll |\Psi(\vec{r})|^2 |\Psi(\vec{r} + \vec{q})|^2 \gg$  of the experimental eigenfunctions is found to be well described [8] by a universal form  $P_2(r) = 1 + cJ_0^2(kr)$ , where  $k$  is the wavevector.  $c$  is a universal constant, with  $c = 2$  in 2-D. Higher order correlations such as joint probability distributions  $P(v_1, v_2)$  which describe correlations of wavefunctions of values  $v_1$  and  $v_2$  were also obtained and found to agree very well with theoretical expectations [9].

These statistical properties of chaotic eigenfunctions are all in good agreement with RMT calculations. The same correlations are also obtained for wavefunctions with Gaussian fluctuations, such as random superpositions of plane waves. Thus these correlations do not contain information regarding classical phase space structures such as periodic orbits, which lead to deviations from these universal functions. Another type of deviations from universal behavior occurs due to localization in disordered systems which is discussed next.

## D: Localization in Disordered Billiards

An entirely new area opens up when experiments are carried out on disordered geometries. Here an additional length scale, the mean free path  $l$ , is introduced by including small metallic scatterers in the cavity. The other relevant length scales are the wavelength  $\lambda$  which can be tuned by varying frequency, and the system size  $L$ . The author and his collaborators first introduced such disordered billiards and directly measured the wavefunctions in them [8].

When  $\lambda \sim l$ , a new phenomenon is observed, *viz.* localization. This is directly observed in the experimental eigenfunctions as shown in Fig.2. The degree of localization can be enormous for certain, relatively rare eigenfunctions. We have carried out extensive analysis of the statistical properties of disordered wavefunctions [8]. The density distribution  $P(|\Psi|^2)$  deviates significantly from the universal P-T distribution discussed above. Localization leads to  $P(|\Psi|^2)$  much larger than the prediction of P-T for large  $|\Psi|^2$ . A quantitative understanding of these distribution functions for disordered geometries is achievable on the basis of theories based on nonlinear sigma models of supersymmetry.

The nonlinear sigma model approach to disordered systems was pioneered by Efetov [21], and is an excellent method for calculating correlations of eigenvalue spectra and eigenfunctions of disordered systems. The model hamiltonian is that of a non-interacting electron in a potential with Gaussian distribution of random disorder. Efetov introduced methods employing supermatrices which enable averages over the disordered potential and yielded correlation functions. The general structure of the theory is worth examining. In the spatially homogeneous zero-mode, or 0D limit, which corresponds to the ballistic limit  $\lambda \ll l$ , the theory reduces to that of the chaotic limit and yields the results of RMT, such as the Porter-Thomas density distribution. The leading term, the 1-mode or 1-D limit, yields the leading corrections due to incipient localization, with higher orders (in principle) leading to increasing localization. Even the 1-D limit becomes very complicated to completely evaluate. However the challenge posed by the experiments [8] appear to have been successfully met by Falko and Efetov [25], who calculated  $P(|\Psi|^2)$  for the 1-mode in spatial 2-D, and are able to fit quantitatively our experimental data with the only parameter needed, the distribution of scatterers, determined by the experimental configuration.

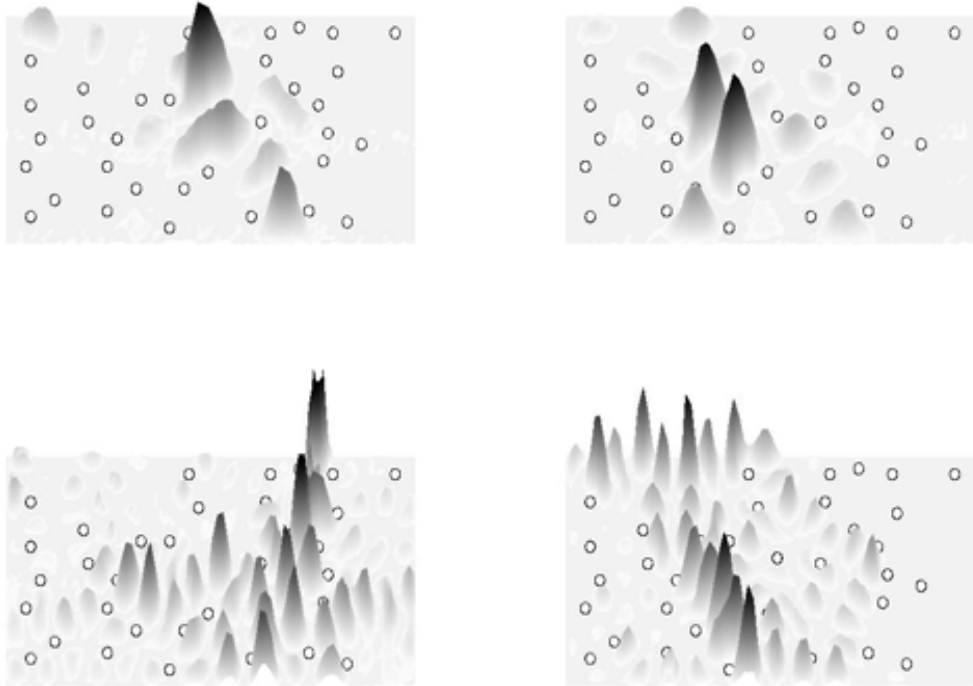


Figure 2: Eigenfunctions of a disordered billiard, directly demonstrating the observation of localization. clockwise, from top left : 3.774 GHz, 3.961 GHz, 6.670 GHz, 6.925 GHz

The degree of localization of eigenfunctions can be best examined by studying the higher moments of the distribution. A particularly useful quantity is the Inverse Participation Ratio (IPR)  $P_2$ , which is the  $n = 2$  member of the series of moments  $P_n = \int |\Psi(\vec{r})|^{2n} d^3r$ . In the chaotic limit,  $P_2 = 1 + c = 3$ , a universal limiting value which is also a direct consequence of the P-T distribution. Indeed we observe an average value 3.0 for the Sinai-Stadium. Marginally stable PO lead to average values 2.75, slightly less than 3, for the Sinai billiard. Note that  $P_2 = 2.25$  for the integrable rectangle. A striking result is that  $P_2$  can become as large as 20 for strongly localized eigenfunctions in the disordered billiards. Indeed we find systematic trends with the IPR  $P_2$  decreasing from large values ( $\sim 20$ ) to the limiting value of 3 as frequency is increased. Thus varying frequency can be used to “tune” the system from “localized” (large IPR) to “metallic” or delocalized (IPR  $\sim 3$ ). This is because increasing  $f$  (decreasing  $\lambda$ ) correspondingly increases a localization length  $\xi$ , which is a monotonically increasing function of the frequency.

There have been several recent results obtained by impressive efforts using the supersymmetry approach [25, 26, 27], partly stimulated by the microwave experiments and by developments in semiconductor microstructures. In particular several calculations have been performed of IPR fluctuations and the properties of the moments  $P_n$ . The ability to obtain localized wavefunctions, and to controllably tune the degree of localization, is a unique advantage of the microwave experiments. Recently we have shown [15] that an important consequence of localization is the observation of level-to-level fluctuations of the Inverse Participation Ratio. Impurity scattering leads to an asymmetric non-Gaussian distribution of the IPR which are observed in the eigenfunctions of the disordered billiards. The experimental results are in quantitative accord with predictions of the non-linear sigma model of supersymmetry [15].

Spatial correlations are of course the key quantity for understanding localization. For incipient localization, the density-density correlator  $P_2(r) \sim 1 + cJ_0^2(kr)$ , however with  $P_2 \equiv P_2(0) = 1 + c > 3$  as noted above. For strongly localized eigenfunctions, where  $P_2 \gg 3$ , the experimental data for  $P_2(r)$  deviate strongly from the universal functional form  $1 + cJ_0^2(kr)$ . Recently we have shown that this quantity decays exponentially with a length scale determined by the mean free path  $l$  [15]. While our results indicate good quantitative descriptions of the data for moderate localization, they also pose challenges to the current status of theory, and will hopefully motivate further (although very demanding) calculations using the nonlinear sigma models for highly localized eigenfunctions.

## E: Open systems : Resonances and decay of a fractal repeller

Recently, we have implemented a new avenue of microwave billiard experiments designed to study model problems in open quantum systems.

The system of  $n$ -disks on a plane is perhaps the simplest and paradigmatic example of a chaotic scattering system. The classical differential cross-section of the system with  $n > 2$  disks on a plane is singular, with singular points forming a Cantor set. Thus, the investigation of chaotic scattering geometries naturally brings in the capability to access the intrinsic *fractal* nature of the underlying classical repeller.

From the perspective of quantum-classical correspondence, the wave-mechanical counterpart of this “fractal pinball game” has received extensive theoretical attention. Semiclassical attempts to treat this problem led to important theoretical advances and to the development of sophisticated semiclassical tools, notably cycle expansion, that represents one of the more productive applications of periodic orbit theory [22].

From a broader perspective,  $n$ -disk scattering can be regarded as the prototype of an *open quantum chaos system*. For closed quantum chaotic systems (billiards in particular), theoretical and experimental results are available on spectral eigenvalues (which are purely real), and a good understanding of both universal and non-universal features has been reached [4]. Open chaotic systems are a special class of open quantum systems, whereby bound states of a closed geometry are converted to long-lived metastable states due to coupling to continua. Accordingly, eigenvalues are intrinsically complex and their universal behavior is currently a subject of considerable interest. In addition, the system turns out to be a good exemplification for a variety of physical situations, ranging from crossroad geometries for semiconductor devices, to electromagnetic and acoustic scattering, and heavy-ion nuclear reactions.

In spite of extensive theoretical investigation, there have been few direct experimental implementations of such chaotic model geometries so far. We have carried out a systematic experimental study of the quantum resonances and decay characteristic of 2-D scattering repellers. The experiments utilize thin microwave geometries where, under appropriate conditions, the underlying Helmholtz equation maps exactly into the time-independent Schrödinger equation in two dimensions. Experiments were carried out for  $n = 1, 2, 3, 4$ , as well as for large  $n = 20$ , the latter corresponding to the so-called random Lorentz scatterer. A concise account of the main results has been presented in [12], and a more detailed description is available in [13].

The experiments, which are able to access the stationary Green’s function of the system, yield the frequencies and the widths of the low-lying quantum resonances. We have carried out semiclassical calculations of such resonances, which are shown to reproduce the measured spectra reasonably well. Our experiments enable us to explore the role of symmetry in a unique way by probing different irreducible representations of the symmetry group of the scatterer. The experimental data are used to identify both universal and non-universal signatures of the classical chaos in the transmission spectra, through measures such as the spectral (wave-vector) autocorrelation function.

Correlation functions are a valuable tool to extract key information on the spectral properties of the system. In mesoscopic conductors, measurements of the magnetic field correlation of the conductivity have provided unique insight into the manifestations of the chaotic classical dynamics at the quantum level. Correlations of wave functions in chaotic systems have been considered recently as a probe for classical ergodicity predictions. In the present experiments, we take advantage of our ability to vary the wave-vector of the system to directly access energy correlations, which are difficult to extract in semiconductor microstructures. The small  $k$  (long time) behavior of the resulting autocorrelation provides a measure of the *quantum escape rate*, which is shown to be in good agreement with the corresponding classical value. For large  $k$  (short time), the contribution of periodic orbits is evidenced through non-universal oscillations of the autocorrelation function.

The connection between so-called transmission function,  $S$ -matrix, and Green’s function is well known in the field of mesoscopic transport. In particular, we recall that the *transmission function* of a coherent

conductor between two leads 1, 2 is defined as  $T = \sum_{m \in 1, n \in 2} |t_{mn}|^2$ , where the transmission coefficient  $t_{mn}$ , which characterizes the transmission amplitude between mode  $m$  in lead 1 and mode  $n$  in lead 2, is given by  $t_{mn} = -i\hbar\sqrt{v_m v_n} \int dy' dy \phi_m^*(y') \phi_n(y) G(y', x_2, y, x_1; k)$ . Here,  $v_m$  ( $v_n$ ) and  $\phi_m$  ( $\phi_n$ ) are the longitudinal velocity and the transverse wave function for the mode  $m$  in lead 1 ( $n$  in lead 2) respectively, while  $x_{1(2)}$  denote the longitudinal coordinate of antennas 1, 2. The transmission coefficients, which are clearly energy (frequency) dependent, are directly related to the correspondent elements of the  $S$ -matrix. In fact, the above expression for  $t_{mn}$  is a two-probe version of the general connection known as the Fisher-Lee relation between the  $S$ -matrix and the Green's function. The transmission  $T$  is related directly to the *conductance*  $\sigma$  of the conductor by the Landauer formula,  $\sigma = (e^2/h)T$ ,  $e$  denoting the electron charge[24].

In the case of a point-like excitation and a point-like probing of the system, the input/output leads act as zero-dimensional tunneling point contacts. Thus, the transverse dimension of the leads can be neglected and the wave functions  $\phi_m(y)$  are proportional to  $\delta$ -functions,  $\phi_m(y') = \delta(y' - y_2)$ ,  $\phi_n(y) = \delta(y - y_1)$ . By combining the two expressions above, and putting  $\vec{r}_1 = (x_1, y_1)$ ,  $\vec{r}_2 = (x_2, y_2)$ , we get  $T(k) \propto |G(\vec{r}_2, \vec{r}_1, k)|^2$ . Since the Green's function is directly related, as shown in the previous section, to the experimental trace, one can interpret  $T(k) \propto |S_{21}(k)|^2$  as a measurement of the two-point conductance. As a consequence, direct comparison is possible with theories originally developed for electronic micro-structures. Note that in the language of mesoscopic conductors, the weak-coupling assumption between the system and the point-like leads implies the possibility of neglecting, as noticed above, any perturbation effect associated with the so-called lead self-energy. From a general point of view, microwave-based implementations offer, compared to their solid-state counterparts, the advantage of a simple and practically unlimited manipulation of geometrical properties, along with the possibility of changing the wave-vector (and thereby the energy) of the incoming waves at will. Lastly, since electromagnetic waves are intrinsically non-interacting, a direct analogy with the ideal limit of a non-interacting electron gas applies and microwave experiments automatically probe quantum transport in the ballistic regime.

The transmission function  $|S_{21}|^2$  for a square 4-disk system with disk radius  $a = 2cm$  and separation  $R = 8cm$  is shown in Fig.1 of ref.[12]. The resonance frequencies  $f$  and widths  $\Delta f$  directly yield the complex wave-vector quantum eigenvalues of the 4-disk repeller. In our previous experiments on closed cavities such as Sinai billiard geometries [1], the widths of the eigen-resonances were due to dissipation in the metal walls. Here however the resonance widths are due to decay of the wavefunction into infinite space. These experiments thus enable us to explore quantum decay in open systems. It must be emphasized that the dissipation in the walls is entirely negligible in the present experiments.

The experimental approach was validated by measurements (not shown) on an (integrable) 2-disk system, for which we have measured both in the full space with two actual disks ( $A_1$  and  $A_2$  representations) and in the half-space using a reflecting mirror ( $A_2$  representation). Here the spectrum consists of a 1-parameter family of resonances due to a single periodic orbit. The experimental data are in very good agreement with semiclassical calculations [13].

For the chaotic 4-disk case, we have also carried out semiclassical calculations using methods in the literature [22]. In the semiclassical theory, the resonances of the system are given by the poles of the Ruelle  $\zeta$  function with  $j$  running from 0 to  $\infty$

$$\zeta_{(1/2)+j}(-ik) = \prod_p \left[ 1 - (-1)^{L_p} \exp(ikl_p) / (\sqrt{\Lambda_p} \Lambda_p^j) \right]^{-1} \quad (2)$$

where  $k$  is the wave vector,  $l_p$  is the length of the periodic orbit  $p$ ,  $L_p$  the number of collisions of the periodic orbit with the disks, and  $\Lambda_p$  is the eigenvalue of the stability matrix.

For the 4-disk system with  $C_{4v}$  symmetry, the semi-classical calculations using the cycle expansions [23] were carried out up to period 3 including 14 periodic orbits. Because of the  $C_{4v}$  symmetry, there are five representations of the Ruelle  $\zeta$  function,  $A_1$ ,  $A_2$ ,  $B_1$ ,  $B_2$ ,  $E$ , where the last one is two-dimensional. The poles of the first Ruelle  $\zeta$  function with  $j = 0$  are calculated, since they contribute to the resonances with the longest lifetimes. The energy of the particle is  $E = k^2$  (here we can take  $m = 1/2$ ,  $\hbar = 1$ ), and is also complex.

The results of the semi-classical calculations, as a superposition of Lorentzians  $S_{cal}^2(k) = \sum_i c_i \gamma_i / ((k - s_i)^2 + \gamma_i^2)$ , where  $s_i$  and  $\gamma_i$  are the calculated real and imaginary parts of resonances, respectively, were compared with experimental data for the transmission spectrum  $S_{21}(k)$  [12, 13]. The coupling constants  $c_i$  were chosen to fit the data - as explained above they are specific to the probe locations. Good agreement is found for the resonance frequencies of the sharp resonances. The sharp resonances with small imaginary parts and hence high  $Q = s_i/\gamma_i \gg 1$ , are easily recognized while the resonances with large imaginary parts

are not easy to distinguish, although all resonances contribute to the transmission function  $S_{21}(k)$ .

The approximate semiclassical theory used provides a fair prediction of the resonance frequencies even for the low-lying resonances. The accuracy is within 5%. But the agreement for the widths is not as good as that for the resonance frequencies. The lower the frequency, the greater the discrepancy between the calculated and experimental widths. The discrepancy may improve if more orbits of higher period are included. Another source of the discrepancy is intrinsic in the semi-classical theory because of the large correction of the stationary phase approximation.

One of the noteworthy features of the experiments is the ability to vary geometry. We exploited this by exploring the role of the symmetry in the 4-disk geometry. We performed the experiment in four different setups. These correspond to four different ways of probing the phase space: the full space in which all five representations are included, half ( $A_2, B_2, E$ ), one fourth ( $B_1, B_2$ ), and one eighth of the space ( $B_2$ ). Approximately 17 configurations were studied and analyzed in details. The systematic trends are consistent with expectations [12, 13].

The spectral auto-correlation function is an important tool to analyze spectra, which was calculated as  $C(\kappa) = \langle |S_{21}(k - (\kappa/2))|^2 |S_{21}(k + (\kappa/2))|^2 \rangle_k$ , is an important tool to analyze spectra. The average is carried out over a band of wave vector centered at certain value  $k_0$  and of width  $\Delta k$ . The window function chosen was  $f(x) = (1 - |x|/\sqrt{6})/\sqrt{6}$  for  $|x| < \sqrt{6}$  and  $f(x) = 0$  for  $|x| \geq \sqrt{6}$  with  $x = (k - k_0)/\Delta k$ . The trace  $S_{21}$  used is the average of several traces collected at different probe locations with the same geometrical configuration of the disks to avoid missing resonances due to the accidental coincidence of either probe with a node of the wavefunction. The autocorrelation is the average of that for several  $k_0$ . A plot of the autocorrelation for the 1/8th configuration of the 4-disk geometry is shown in [12, 13].

Since  $|S_{21}(k)|^2 = \sum_i c_i \gamma_i / ((k - s_i)^2 + \gamma_i^2)$ , we have  $C(\kappa) = \pi \sum_{i,j} c_i c_j (\gamma_i + \gamma_j) / ((\kappa - (s_i - s_j))^2 + (\gamma_i + \gamma_j)^2)$ . In the case that there are no overlapping resonances,  $|s_i - s_j| \gg (\gamma_i + \gamma_j)$ , the small  $\kappa$  behavior of the autocorrelation is  $C(\kappa) \approx \pi \sum_i 2c_i^2 \gamma_i / (\kappa^2 + 4\gamma_i^2)$ .

According to semiclassical theory, the above sum can be replaced by a single Lorentzian

$$C(\kappa) = C(0) \frac{1}{1 + (\kappa/\gamma)^2}. \quad (3)$$

In semi-classical theory,  $\gamma = \gamma_0$ , the classical escape rate with the velocity scaled to 1. Thus one can interpret the width of the autocorrelation as an average lifetime of resonances. The above equation was used to fit the spectral autocorrelation for small  $\kappa$  and thus obtain the value of the experimental escape rate  $\gamma_{qm}$ , as shown in Fig.2 of ref.[12].

In the classical scattering theory, the classical escape rate  $\gamma_0$  is the simple pole of the classical Ruelle  $\zeta$  function. We use the results of ref.[22] for comparison with the experimental data. Asymptotically, when  $R$  is large,  $\gamma_0 \approx \ln(2\sqrt{2}R/a)/(\sqrt{2}R)$ . Another relevant quantity is the abscissa of absolute convergence  $s_c$  which can also be estimated from the Ruelle  $\zeta$  function with the classical cycle weights  $t_p$  replaced by the corresponding semiclassical ones.  $s_c$  serves as a lower bound of the escape rate.

Good agreement of the escape rate is obtained between that of the classical theory  $\gamma_0$  and that from the experimental data  $\gamma_{qm}$ . This is shown in Fig.3 of ref.[12], where we compare the experimental escape rates  $\gamma_{qm}$  with the classical escape rate  $\gamma_0$  for several values of  $R/a$ . Note that data were obtained for 17 configurations of the different reduced (1/8, 1/4, 1/2 and full space) representations of the 4-disk geometry. The radius of the disks used was  $a = 5cm$  for the 1/8 space, and  $a = 2cm$  for the others. The data for  $\gamma_{qm}$  are scaled to radius  $a = 1$ . We have thus shown experimentally that the small  $\kappa$  behavior of the spectral auto-correlation has a universal behavior in that it is independent of the details of the geometry. The good agreement between the measured escape rate  $\gamma_{qm}$  and the classical escape rate  $\gamma_0$  shows that some quantum properties are well predicted by semiclassical theory.

## F: Tunneling

Tunneling and dissipation are ubiquitous phenomena in physics. A detailed understanding of their combined action would be highly desirable given the relevance of the problem for atomic physics, condensed matter physics, chemistry and biology [28]. However, the incorporation of dissipative effects is by no means trivial. Due to limitations of the available analytical and computational methods, up-to-date descriptions are mainly restricted to a few manageable cases, the prototype situation involving a bistable potential in 1D.

We recently observed some novel aspects of tunneling in 2D potentials and its interplay with classical dissipation. In experiments utilizing microwave dielectric resonators, we find that symmetry not only plays



a crucial role while shaping the eigenstates of the system, but also influences the way they couple to the external environment acquiring a finite width. In the observed resonance multiplets, we find that one of the members is extremely sharp due to the symmetry of the configuration. The large ratios of the observed widths appear to be a peculiar consequence of the multidimensional nature of the system. A detailed description of the experimental results and analysis is presented in ref.[16].

The experiments were carried out using MgTi dielectric cylinders placed between two parallel copper plates, 30 cm square, separated by a gap  $l = 6.38$  mm. The disks had diameter  $D = 12.65$  mm and dielectric constant  $\epsilon_r = 16$ . After establishing input/output coupling to the *near* field of the resonators by inserting coax lines terminated by loops, measurements of the transmission amplitude as a function of the frequency were performed using an HP8510B network analyzer.

When two dielectric resonators are placed *in proximity* to each other, each resonance splits into two. The doublets have the structure of a *broad resonance at a lower frequency*  $f_l$  accompanied by a *narrow resonance at higher frequency*  $f_h$ . This effect is particularly pronounced for TM modes ( $H_z = 0$ ). The most noteworthy example is the  $TM_{011}$  single-disk resonance found at 9.45 GHz with  $Q_0 \approx 70$ , which splits into two peaks with  $Q_h \approx 2400$  and  $Q_l \approx 50$  for an edge distance  $d = 1.0$  mm. The narrow peak can be experimentally assigned to an *antisymmetric*  $E_z$ -field configuration by establishing electric field coupling with the pick-up antenna and by probing the behavior at the mirror symmetry plane. The doublet splitting as a function of the disk separation  $\Delta f(d) = f_h - f_l$  vanishes exponentially with separation  $d$  until the limit of noninteracting resonators is approached. The measured decay constant is in good agreement with the single-disk value  $\kappa_r = 0.45$  mm $^{-1}$ , as expected on the basis of semiclassical estimates in a tunneling regime where  $\kappa_r d \geq 1$  [29]. The widths  $\gamma_l, \gamma_h$  and their ratio  $\gamma_l/\gamma_h$  are plotted in Fig. 3(b) and in Fig. 4 of ref.[16] respectively. Again, single-disk behavior is recovered for sufficiently large  $d$ , where  $\gamma_l, \gamma_h \rightarrow \gamma_0$ . For small separations, the width  $\gamma_h$  is highly suppressed, leading to the high  $Q$ -values noted above. As indicated by Fig. 4 of ref.[16], a maximum ratio  $\gamma_l/\gamma_h \approx 50$  is seen at  $d = 0.73$  mm. It is very remarkable that, thanks to the proximity effect,  $Q$ 's in the range of  $10^3$  are achievable without resorting to closed-walls cavities.

Our results have a variety of implications. First, the tunneling interaction in a 2D integrable potential has been probed sensitively. There is no difficulty, in principle, to extend the experimental work to chaotic potentials where important results on complex periodic orbits theory have been obtained [29]. Second, the experiments demonstrate how symmetry properties can be usefully exploited to protect a system against the effects of its environment. This general mechanism provides a unifying explanation for proximity resonances, regardless of the unbound (scattering) or bound (confined) nature of the wave field. Third, it is conceivable that some counterpart of proximity phenomena may be relevant on the mesoscopic scale as well. From the practical perspective, the possibility of symmetry-based  $Q$ -amplification in electromagnetic or photonic structures represents another exciting area of applications. Finally, the electromagnetic phenomenon evidenced here displays intriguing similarities with concepts investigated in the context of quantum dissipative processes. The possibility of establishing a mapping between the electromagnetic and quantum realm even in the presence of dissipative mechanisms would clearly open up a fruitful arena of interchange and deserves further investigation.

## G: Summary and Conclusions

A vast array of issues in Quantum Chaos, Localization and even Tunneling can be addressed by well-planned microwave experiments. In addition to the topics discussed here, other areas which we plan to address are parametric variation of eigenvalues and eigenfunctions, and chaos-assisted tunneling.

Support for this research from NSF-PHY-9722681 is gratefully acknowledged. The author thanks his principal collaborators A.Kudrolli, K.Pance, W.T.Lu, M.Rose, P.Pradhan and V.Kidambi for their numerous contributions. S.S. thanks the hospitality provided during the Quantum Chaos Workshop at the Australian National University, Canberra.

## References

- [1] S. Sridhar, Phys. Rev. Lett., **67**, 785 (1991)
- [2] S. Sridhar, D. Hogenboom and Balam A. Willemsen, J. Stat. Phys. , **68**, 239 (1992).
- [3] S. Sridhar, D. Hogenboom and A. Kudrolli, in "Quantum Non-Integrability", ed. by D. H. Feng, J. M. Yuan and G. Zaslavsky, (Gordon & Breach , 1993).

- [4] A. Kudrolli, S. Sridhar, A. Pandey and R. Ramaswamy, Phys. Rev. E. (Rapid Comm.) , **49**, R11 (1994).
- [5] S. Sridhar and E. J. Heller, Phys. Rev. A , **46**, R1728 (1992).
- [6] S. Sridhar and A. Kudrolli, Phys. Rev. Lett. , **72**, 2175 (1994).
- [7] S. Sridhar, D. Hogenboom and A. Kudrolli , in “Quantum Non-Integrability”, ed. by D. H. Feng, J. M. Yuan and G. Zaslavsky, (Gordon & Breach, 1993).
- [8] A. Kudrolli, V. Kidambi and S. Sridhar, Phys. Rev. Lett., **75**, 822 (1995).
- [9] V. Prigodin, N. Taniguchi, A. Kudrolli, V. Kidambi and S. Sridhar, Phys. Rev. Lett. , **75**, 2392-2395 (1995).
- [10] A. Kudrolli and S. Sridhar, Phys. Rev. Lett., **76**, 3036 (1996).
- [11] A. Kudrolli and S. Sridhar, Pramana: Special Issue on Chaos, **48**, 459 (1997).
- [12] Wentao Lu, M. Rose, K. Pance and S.Sridhar, Phys. Rev. Lett., **82**, 5233 (1999)
- [13] Wentao Lu, Lorenza Viola, Kristi Pance, Michael Rose, S. Sridhar, Phys. Rev. E, (2000, to appear).
- [14] K.Pance, W.T.Lu and S.Sridhar, Phys. Rev. Lett., (submitted).
- [15] P.Pradhan and S.Sridhar, Phys. Rev. Lett., (submitted).
- [16] K.Pance, L.Viola and S.Sridhar, Phys. Lett. A., (2000, to appear).
- [17] M. C. Gutzwiller, Chaos in Classical and Quantum Mechanics (Springer-Verlag, New York, 1990).
- [18] M.L.Mehta, “Random Matrices”, (Academic Press, 1991).
- [19] O. Bohigas, M. J. Giannoni and C. Schmit, Phys. Rev. Lett. **52**, 1 (1984).
- [20] E. J. Heller, Phys. Rev. Lett. **53**, 1515 (1984).
- [21] K. B. Efetov, *Supersymmetry in Disorder and Chaos* (Cambridge University press, 1997).
- [22] P. Gaspard, “*Chaos, scattering and statistical mechanics*”, Cambridge University(1998).
- [23] P. Cvitanović, R. Artuso, R. Mainieri, and G. Vattay, *Classical and Quantum Chaos: a Cyclist Treatise* (unpublished, 1998).
- [24] S. Datta, *Electronic Transport in Mesoscopic Systems* (Cambridge University Press, Cambridge, 1995).
- [25] V. Falko and K. Efetov, Phys. Rev. B **50**, 954(1994).
- [26] A.Mirlin, Advances in Physics, (2000, to appear).
- [27] V.Prigodin and B.Altshuler, Phys. Rev. Lett. **80**, 11267 (1998).
- [28] J. Jortner and B. Pullman, *Tunneling* (Reidel, Dordrecht, 1986).
- [29] S. C. Creagh and N. D. Whelan, Phys. Rev. Lett. **77**, 4975 (1996).